New Anisoparametric 3-Node Elements for Out-of-Plane Deformable Curved Beam

Kim Moon-joon, Min Oak-key*
Department of Mechanical Design & Production Engineering, Yonsei University
Kim Yong-woo
Department of Mechanical Engineering, College of Engineering, Sunchon National Universoty
Moon Won-joo
Senior Research Engineer, OEM Development Team, R & D Center, Hankook Tire Corporation

Based on numerical reduced minimization theory, new anisoparametric 3-node elements for out-of-plane curved beam are developed. The elements are designed to be free from spurious constraints. In this paper, the effect of the Jacobian upon numerical solution is analyzed and predicted through reduced minimization analysis of anisoparametric 3-node elements with different Jacobian assumption. The prediction is verified by numerical tests for circular and spiral out-of-plane deformable curved beam models. This paper proposes two kinds of 3-node elements with 7-DOF; one element employs 2-point integration for all strains, and the other element uses 3-point integration with a constant Jacobian within element for calculation of shear strain.

Key Words : Numerical Reduced Minimization Theory, Anisoparametric 3-node Element, Jacobian, Spurious Constraint, Locking

1. Introduction

Many investigators have studied curved beam finite elements to improve the convergence and accuracy for last thirty years. Looking into their studies, the main cause of error when using C^0-continuous elements in finite element analysis, is known as a stiffness locking phenomenon. The locking phenomenon is characterized by two typical numerical behaviors in a static analysis; one is a much smaller displacement than the exact one, and the other is the violent undulate stress distributions. As a result of these intensive studies, they have revealed that an inconsistent assumption on displacement functions produces spurious constraints when full integration is employed. Many remedies of the stiffness locking have been studied. The uniformly/selectively reduced integration proposed by Zienkiewicz (1989) has been used for the representative remedies for locking. Tessler (1986, 1988) has developed an anisoparametric element that has different numbers of nodes depending on strain component. Prathap and Babu (1986) explained how the full integration for shear and extensional strain energy leads to locking, and removed the cause by using the modified shape functions in order not to yield any spurious constraints. Kamoulakos (1988) explained how reduced integration yields improved results by illustrating a simple example. Min and Kim (1993, 1994, 1995, 1996) have explained the role of a reduced integration from the viewpoint of minimization. They have clarified the relationship amongst spurious constraints, optimal points, and integration order by using the reduced minimization theory.

* Corresponding Author,
E-mail : minokey@bubble. yonsei. ac. kr
TEL : +82-2-361-2817 ; **FAX** : +82-2-362-2736
Department of Mechanical Design & Production Engineering, College of Engineering, Yonsei University, 134, Shinchon-dong, Seodaemun-ku, Seoul 120-749, Korea. (Manuscript **Received** March 24, 1999 ; **Revised** October 20, 1999)

Recently, Sengupta and Dasgupta (1997) have used a five-node thirteen DOF anisoparametric element using different degrees of polynomials for interpolating deflection and rotations, and have shown coincidence of numerical solutions and exact ones for various models including a curved beam with a spiral geometry. However, they have not mentioned why their element has a locking-free property.

In this paper, we present new 3-node anisoparametric elements which have similar formulation procedure as Sengupta's 5-noded element and we show why the new elements have locking-free property by deriving the new elements based on reduced minimization theory. Additionally, because the elements are defined by using global Cartesian coordinates, their Jacobian cannot be constant. This can be a cause of locking (Min and Kim, 1996). Thus, we analyze the combined effect of Jacobian and integration rule used upon numerical solutions to design locking-free elements. We present typical numerical tests to examine the performance of the new elements and to verify the analysis used in this paper.

2. Anisoparametric Three-Node Element

Sengupta (1997) employed a 5-node thirteen DOF horizontally curved beam element with different degrees of interpolating polynomials. One set is a fourth-degree Lagrangian polynomial, which is used for interpolating out-of-plane-deformable curved beam geometry and vertical displacement, and another is a third-degree polynomial, which is used for the angles of bending rotation and twisting rotation. A similar procedure can be applied to 3-node element.

2.1 Geometry and displacements

The geometry of a 3-node out-of-plane deformable curved beam element, which is in x-y plane as shown in Fig. 1(a), is represented by

$$x=\sum_{i=1}^{3}x_iN_{wi} \text{ and } y=\sum_{i=1}^{3}y_iN_{wi} \tag{1}$$

where $N_{w1}=\frac{1}{2}\xi(\xi-1)$, $N_{w2}=(1+\xi)(1-\xi)$,

$$N_{w3}=\frac{1}{2}\xi(\xi+1) \tag{2}$$

In Eq. (2), $\xi(\in[-1, +1])$ is one-dimensional natural coordinate as shown in Fig. 1(b).

In Fig. 1(a), s is the curvilinear coordinate running along the neutral axis of a curved beam and **t**-**n**-**b** is the trihedron of the curved beam at a point on s, where **t** is unit tangent vector, **n** is unit principal normal vector and **b** is unit binormal vector (1983, Kreyszig).

The binormal deflection (w) is interpolated by the same shape functions N_{wi}.

$$w=\sum_{i=1}^{3}N_{wi}w_i \tag{3}$$

The angles of twisting and bending rotations (θ_t and θ_n) are interpolated by a new set of shape functions $N_{\theta i}$

$$\theta_t=\sum_{i=1,i\neq 2}^{3}N_{\theta i}\theta_{t_i}$$
$$\theta_n=\sum_{i=1,i\neq 2}^{3}N_{\theta i}\theta_{n_i} \tag{4}$$

where $N_{\theta 1}=(1-\xi)/2$, $N_{\theta 3}=(1+\xi)/2$ (5)

2.2 Strain definition of out-of-plane-deformable curved beam

The energy of an out-of-plane-deformable curved beam is given by

$$U=\frac{1}{2}\int_s\{GAk_b(\gamma_n)^2+GK(\chi_t)^2+EJ_n(\chi_n)^2\}ds \tag{6}$$

where E is the Young's modulus, G is the shear modulus, K is the polar moment of inertia, GK is the torsional rigidity, A is the cross-sectional area, J_n is the second moment of area, k_b is **b**-directional shear correction factor, γ_n is the shear strain, χ_t is the twisting strain and χ_n is a bending strain.

Displacements and stresses of out-of-plane-deformable curved beam are shown in Fig. 1(c). The displacements vector **u** on the any point of the beam axis can be expressed as:

$$\mathbf{u}=\begin{Bmatrix}\mathrm{w}\\ \theta_t\\ \theta_n\end{Bmatrix}=\mathbf{N}\boldsymbol{\delta}=[\mathbf{N}_1\ \mathbf{N}_2\ \mathbf{N}_3]\begin{Bmatrix}\mathbf{w}\\ \boldsymbol{\theta}_t\\ \boldsymbol{\theta}_n\end{Bmatrix} \tag{7}$$

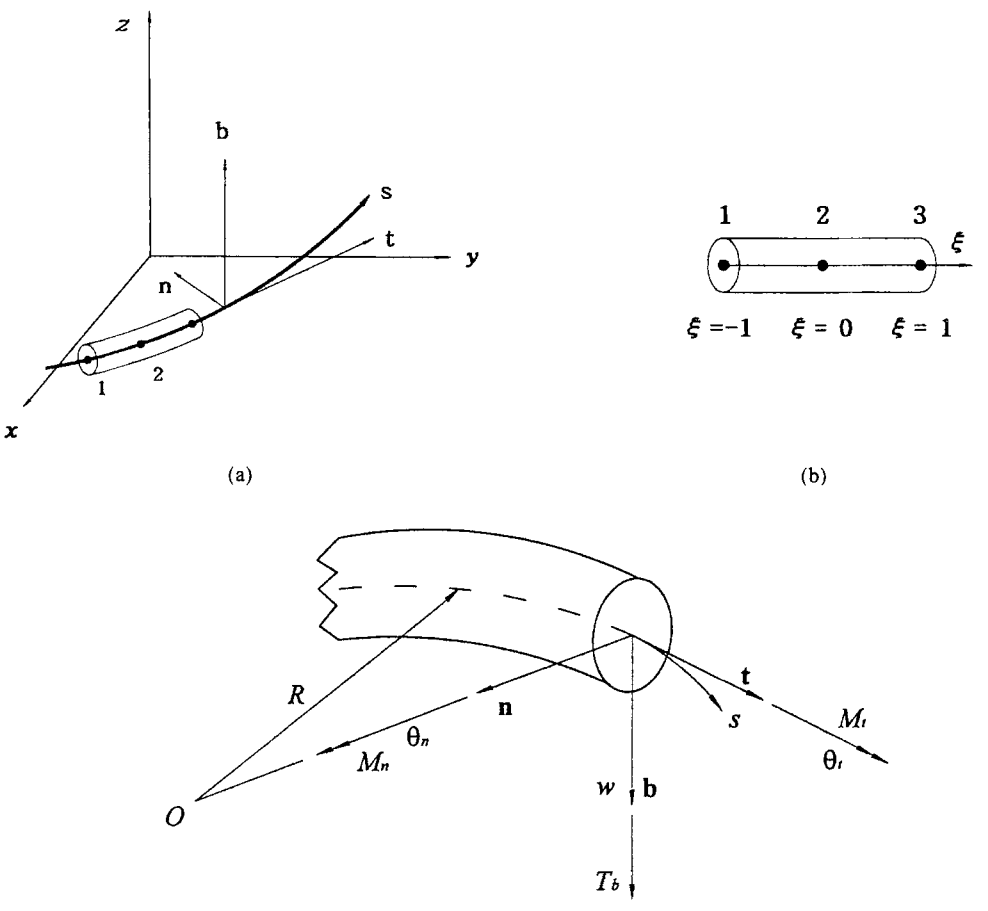

Fig. 1 (a) Curvilinear coordinate systems in 3-dimensional space
(b) A 3-node curved beam element in natural coordinate
(c) Positive sense of generalized displacements and stresses

$$\text{where } \mathbf{N}_1=\begin{bmatrix} N_{w1} & N_{w2} & N_{w3} \\ 0 & 0 & 0 \\ 0 & 0 & 0 \end{bmatrix},\ \mathbf{N}_2=\begin{bmatrix} 0 & 0 \\ N_{\theta 1} & N_{\theta 3} \\ 0 & 0 \end{bmatrix},$$

$$\mathbf{N}_3=\begin{bmatrix} 0 & 0 \\ 0 & 0 \\ N_{\theta 1} & N_{\theta 3} \end{bmatrix}$$

$$\mathbf{w}=\begin{Bmatrix} w_1 \\ w_2 \\ w_3 \end{Bmatrix},\ \boldsymbol{\theta}_t=\begin{Bmatrix} \theta_{t1} \\ \\ \theta_{t3} \end{Bmatrix},\ \boldsymbol{\theta}_n=\begin{Bmatrix} \theta_{n1} \\ \\ \theta_{n3} \end{Bmatrix},\ \boldsymbol{\delta}=\begin{Bmatrix} \mathbf{w} \\ \boldsymbol{\theta}_t \\ \boldsymbol{\theta}_n \end{Bmatrix} \tag{8}$$

The strains of out-of-plane-deformable curved beam are defined as (Moon et. al., 1996)

$$\boldsymbol{\varepsilon}=\begin{Bmatrix} \gamma_n \\ \chi_t \\ \chi_n \end{Bmatrix}=\begin{Bmatrix} \dfrac{dw}{ds}+\theta_n \\ \dfrac{d\theta_t}{ds}-\chi\theta_n \\ \dfrac{d\theta_n}{ds}+\chi\theta_t \end{Bmatrix}$$

$$=\begin{bmatrix} \dfrac{d}{ds} & 0 & 1 \\ 0 & \dfrac{d}{ds} & -\chi \\ 0 & \chi & \dfrac{d}{ds} \end{bmatrix}\begin{Bmatrix} w \\ \theta_t \\ \theta_n \end{Bmatrix}=\mathbf{Lu} \tag{9}$$

where χ is a curvature at a point (x, y) on the beam and it is given by

$$\varkappa=\frac{d^2y/dx^2}{[1+(dy/dx)^2]^{3/2}} \tag{10}$$

The curvature is calculated by using Eq. (1).

Using Eqs. (7) and (8), we obtain strain-displacement matrix $\mathbf{B}(3\times 7)$.

$$\varepsilon=\mathbf{LN}\delta=\mathbf{B}\delta=[\mathbf{B}_1\ \mathbf{B}_2\ \mathbf{B}_3]\begin{Bmatrix}\mathbf{w}\\ \theta_t\\ \theta_n\end{Bmatrix} \tag{11}$$

where

$$\mathbf{B}_1=\begin{bmatrix}N_{w1,s} & N_{w2,s} & N_{w3,s}\\ 0 & 0 & 0\\ 0 & 0 & 0\end{bmatrix}$$

$$\mathbf{B}_2=\begin{bmatrix}0 & 0\\ N_{\theta 1,s} & N_{\theta 3,s}\\ \varkappa N_{\theta 1} & \varkappa N_{\theta 3}\end{bmatrix}$$

$$\mathbf{B}_3=\begin{bmatrix}N_{\theta 1} & N_{\theta 3}\\ -\varkappa N_{\theta 1} & -\varkappa N_{\theta 3}\\ N_{\theta 1,s} & N_{\theta 3,s}\end{bmatrix} \tag{12}$$

2.3 Stress-strain relationship

The stresses, viz., shear force(T_b), bending moment(M_n) and twisting moment(M_t) at any section are expressed as follows(Moon et. al., 1996):

$$\begin{aligned}T_b&=GAk_b(w_{,s}+\theta_n)\\ M_t&=GK(\theta_{t,s}-\varkappa\theta_n)\\ M_n&=EJ_n(\theta_{n,s}+\varkappa\theta_t)\end{aligned} \tag{13}$$

3. Numerical Reduced Minimization Theory

For a curved beam of a circular cross section with a constant diameter d, consider the strain energy

$$U'=\frac{GAk_b}{EJ_n}\int_s(\gamma_n)^2ds+\frac{GK}{EJ_n}\int_s(\chi_t)^2ds+\int_s(\chi_n)^2ds \tag{14}$$

which is obtained by dividing Eq. (6) by $EJ_n/2$. The relation in Eq. (14) shows the relative importance of the shearing, twisting and bending contributions to the element stiffness of a C^0-continuous finite element. The shearing, twisting and bending contributions are represented by the first, the second and the third terms on the right hand side of Eq. (14), respectively. When $d\to 0$. $(GAk_b/EJ_n)\to\infty$ and $(GK/EJ_n)\to 1/4(1+\nu)$ where ν is Poisson's ratio. This indicates that the factor GAk_b/EJ_n in the shearing term can be very large when a thin beam is considered. This factor can be interpreted as a penalty factor. Thus, the shear strain energy is a constrained energy and bending and twisting energies are unconstrained ones. As the beam becomes thin, the constraint of zero shear deformation, i. e., $\gamma_n=\theta_n+dw/ds=0$ will be approached and the deformation is governed by the shear constraint. If the zero shear constraint is not satisfied, the spurious energy cause shear locking when the low-order elements are used(Prathap et. al., 1986, 1987, 1990).

In reduced minimization theory, the above fact is shown through the minimization of the total strain energy which is consists of constrained and unconstrained energy, that is, for the minimization of total strain energy to satisfy the zero shear constraint, the minimization of the constrained energy should not produce any spurious constraints. Since the reduced minimization theory can be found in other publications(Min and Kim, 1991, 1994~1997), instead of repeating a mention on it, we present two conclusive theorems of the numerical reduced minimization theory, which is obtained by minimization of the constrained energy: The constrained shear strain can be expressed as

$$\begin{aligned}\gamma_n&=\theta_n(\xi)+\frac{dw(\xi)}{ds}\\ &=\theta_n(\xi)+\xi_{,s}\frac{dw(\xi)}{d\xi}\end{aligned} \tag{15}$$

where $\theta_n(\xi)$ and $w(\xi)$ are displacement functions defined in element coordinate ξ. We will use two theorems in this paper: one is the theorem for the uniform isoparametric mapping when $\xi_{,s}$ is constant, the other one is the theorem for the non-uniform isoparametric mapping when $\xi_{,s}$ is not constant.

3.1 Numerical minimization under uniform isoparametric mapping (Min and Kim, 1994)

When the displacements are approximated by

complete polynomials of degree $(n-1)$, the constrained strain is expressed as

$$\gamma_n = A_0 + A_1\xi + \cdots + A_{n-3}\xi^{n-3} + A_{n-2}\xi^{n-2} + A^*_{n-1}\xi^{n-1} \quad (16)$$

where A^*_{n-1} is the unmatched coefficient and A_k $(k=0, 1\cdots n-3, n-2)$ are matched coefficients.

The error-moment equations that minimize the constrained strain energy are given as

$$\int_{-1}^{+1} \gamma_n \xi^{k-1} d\xi \langle n : H\rangle = 0, \; k=1, 2, 3, \cdots, H \quad (17)$$

where H is number of integration points used.

(1) If $H \geq n$, then the n error-moment equations produce one spurious constraint and $(n-1)$ independent true constraints.

(2) If $H \leq n-1$, then the $(n-1)$ error-moment equations produce no spurious constraints but yield H independent true constraints only.

3.2 Reduced minimization under non-uniform mapping (Min and Kim, 1996)

When the displacements are approximated by complete polynomials of degree $(n-1)$, and mapping function is assumed by complete polynomials of degree m, the constrained strain (γ_n) is expressed as

$$\gamma_n = \xi_{,s}\overline{\gamma_n} = \xi_{,s}(A_0 + A_1\xi + \cdots + A_{n-2}\xi^{n-2} + A^*_{n-1}\xi^{n-1} + A^*_n\xi^n + \cdots + A^*_{n+m-1}\xi^{n+m-1}) \quad (18)$$

where $\overline{\gamma_n} = A_0 + A_1\xi + \cdots + A_{n-2}\xi^{n-2} + A^*_{n-1}\xi^{n-1} + A^*_n\xi^n + \cdots + A^*_{n+m-1}\xi^{n+m-1}$

$A_k(k=0, 1, \cdots, n-2)$ are matched coefficients, and $A^*_k(k=n-1, n, \cdots, n+m-1)$ are unmatched coefficients.

The error-moment equations that minimize the constrained strain energy by using H-point Gaussian quadrature are given as

$$\int_{-1}^{+1} \overline{\gamma_n} \xi^{k-1} d\xi \langle n : H\rangle = 0, \; k=1, 2, 3, \cdots, H \quad (19)$$

(1) If $H \geq n+m$, then the error-moment equations in Eq. (19) produce $(n-1)$ true constraints and $(m+1)$ spurious constraints.

(2) If $n+m > H \geq n$, then H error-moment equations produce $(n-1)$ true constraints and $(H-n+1)$ spurious constraints.

(3) If $H \leq n-1$, then H error-moment equations produce no spurious constrains but yield H true constraints only.

From the above theorems, $(n-1)$-point minimization or integration can be considered as an optimal minimization or integration since the $(n-1)$-point minimization produces maximum number of true constraints without spurious constraints. Namely, when using n-node element, $(n-1)$-point integration is optimal integration regardless of isoparametric mapping or anisoparametric mapping.

4. Application of Reduced Minimization Theory

4.1 Consideration of Jacobian

The Jacobian calculated in the Cartesian coordinates are expressed as

$$J = \frac{ds}{d\xi} = \sqrt{\left(\sum_{i=1}^{n} \frac{dN_{wi}}{d\xi} x_i\right)^2 + \left(\sum_{i=1}^{n} \frac{dN_{wi}}{d\xi} y_i\right)^2} \quad (20)$$

It should be noted that Jacobian calculated by Eq. (20) cannot be constraint unless the geometry of a beam is straight.

To clarify the relationship between integration points and stiffness locking due to spurious constraint, we will employ the numerical reduced minimization theory under non-uniform mapping. To use the theory, Jacobian in Eq. (20) should be expressed in terms of polynomial. Thus, instead of Eq. (20), we will use a fitted Jacobian which is obtained by using least squares fit. Using the fitted Jacobian, we will apply $(n-1)$-and n-point minimization to the shear strain energy.

4.1.1 Jacobian of circularly-curved beam

The curved beam shown in Fig. 2(a) has an opening angle $\pi/2$, a circular cross-section with diameter $d=0.05m$, and radius of curvature $R=5m$.

When the beam is discretized by a single 3-noded element as shown in Fig 2(b), the fitted

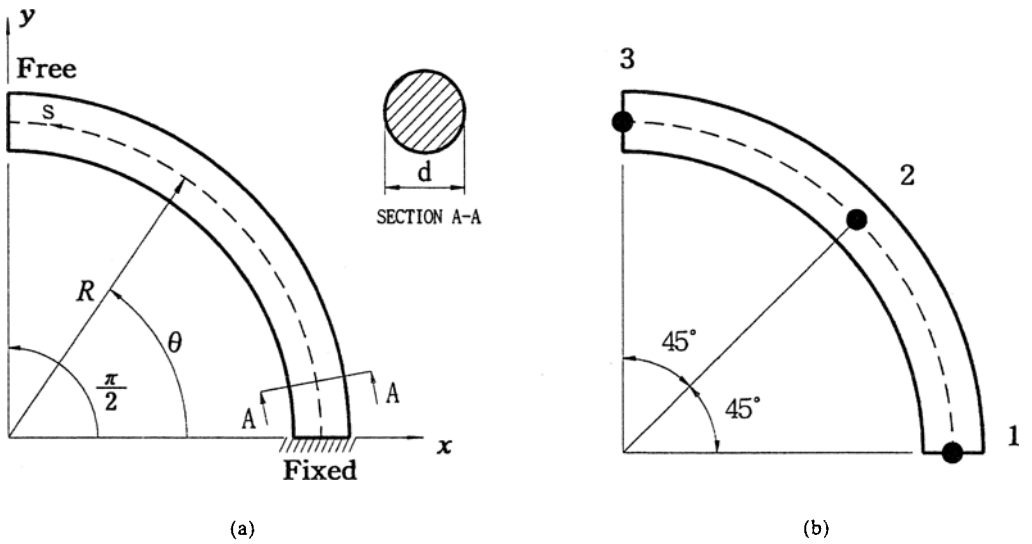

(a) (b)

Fig. 2 (a) An out-of-plane deformable curved beam with a circular geometry; the radius of curvature $R=5m$ and $d=0.05m$
(b) Discretization by a single 3-node element

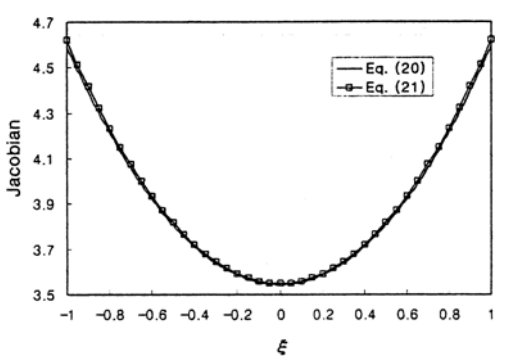

Fig. 3 Jacobian of the out-of-plane deformable curved beam with a circular geometry when single element is used

Jacobian is

$$J_{fit}=1.07147\xi^2+3.54874 \tag{21}$$

which is plotted in Fig. 3 together with Eq. (20).

4.1.2 Jacobian of spiraly-curved beam

The curved beam shown in Fig. 4(a) has an open angle $\pi/2$, and a circular cross-section with its diameter $d=0.05m$. Its radius of curvature is given by $R=R_0\left\{1-\mu(\frac{\pi}{2}-\theta)\right\}$, $(0\le\theta\le\pi/2)$ where $R_o=5m$ and $\mu=0.2$.

When the beam is discretized by a single 3-noded element as shown in Fig. 4(b), the fitted Jacobian is expressed as

$$J_{fit}=1.01926\xi^2-0.53285\xi+3.04313 \tag{22}$$

which is plotted in Fig. 5 together with Eq. (20).

4.2 Application of numerical reduced minimization theory

The constrained strain of out-of-plane-deformable curved beam is expressed as

$$\gamma_n=\frac{dw}{ds}+\theta_n$$
$$=\frac{1}{J}\overline{\gamma_n} \tag{23}$$

where, $\overline{\gamma_n}=w_{,\xi}+J\theta_n$ (24)

When employing 3-node anisoparametric element, the binormal displacement w and the rotation θ_n are approximated as follows.

$$w=a_0+a_1\xi+a_2\xi^2$$
$$\overline{\theta_n}=\overline{b_0}+\overline{b_1}\xi \tag{25}$$

Using Eq. (25), the $\overline{\gamma_n}$ is expressed as

$$\overline{\gamma_n}=(a_1+2a_2\xi)+J(\overline{b_0}+\overline{b_1}\xi) \tag{26}$$

4.2.1 When Jacobian is constant

If the Jacobian is constant, i. e., $J=a_0$, Eq. (26) can be written as

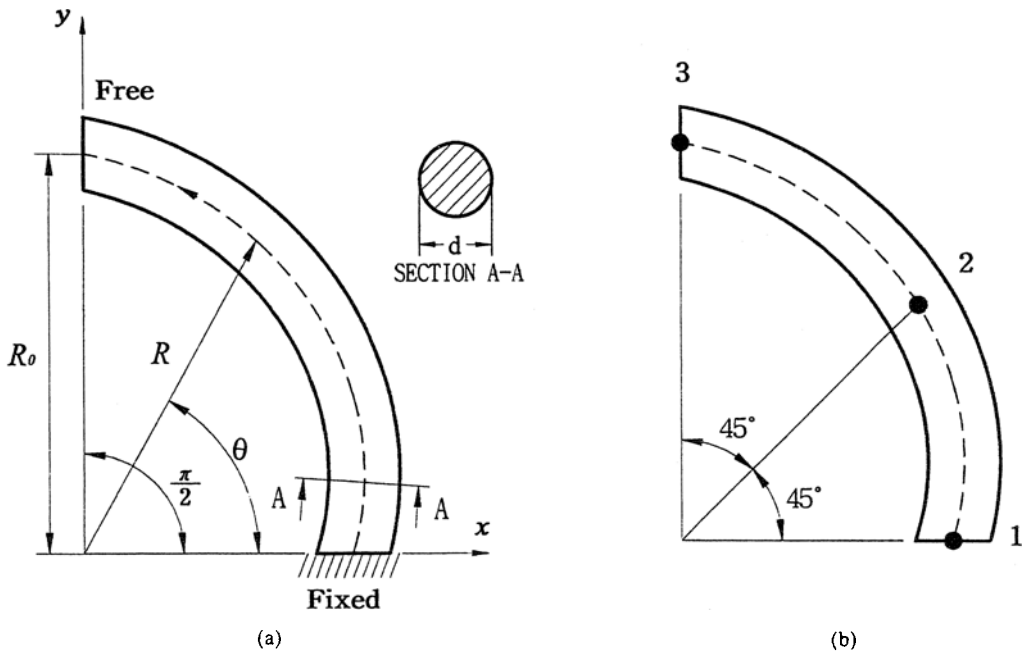

Fig. 4 (a) An out-of-plane-deformable curved beam with a spiral geometry; the radius of curvature $R=R_0\{1-\mu(\pi/2-\theta)\}$ where $R_0=5m$, $\mu=0.2$ and $d=0.05m$
(b) Discretization by a single 3-node element

$$\overline{\gamma_n}=\overline{A_0}+\overline{A_1}\xi \tag{27}$$

where, $\overline{A_0}=a_1+\alpha_0\overline{b_0}$, and $\overline{A_1}=2a_2+\alpha_0\overline{b_1}$

Since the $\overline{\gamma_n}$ is expressed only by matched coefficients ($\overline{A_0}$, $\overline{A_1}$), no spurious constraints are produced. Thus, if we set Jacobian constraint, the numerical solutions will be free from spurious constraints.

4.2.2 When Jacobian is approximated by polynomials

Considering Eqs. (21) and (22), assume

$$J=J_{fit}=\alpha_0+\alpha_1\xi+\alpha_2\xi^2 \tag{28}$$

where $\alpha_i(i=0, 1, 2)$ are some constraints.

Using Eq. (28), $\overline{\gamma_n}$ in Eq. (26) is expressed as

$$\overline{\gamma_n}=\overline{A_0}+\overline{A_1}\xi+\overline{A_2^*}\xi^2+\overline{A_3^*}\xi^3 \tag{29}$$

where

$$\overline{A_0}=a_1+\alpha_0\overline{b_0}$$
$$\overline{A_1}=2a_2+\alpha_0\overline{b_1}+\alpha_1\overline{b_0}$$
$$\overline{A_2^*}=\alpha_1\overline{b_1}+\alpha_2\overline{b_0}$$
$$\overline{A_3^*}=\alpha_2\overline{b_1}$$

When 2-point minimization (or integration) is employed, the error-moment equations for the minimization of the constrained strain energy are given, from Eq. (19), by

$$\int_{-1}^{1}\overline{\gamma_n}d\xi\langle 3:2\rangle=0$$
$$\int_{-1}^{1}\overline{\gamma_n}\xi d\xi\langle 3:2\rangle=0 \tag{30}$$

These equations produce following true constraints,

$$\overline{A_0}+\overline{A_2^*}(^2\xi_1)^2=0$$
$$\overline{A_1}+\overline{A_3^*}(^2\xi_1)^2=0 \tag{31}$$

where $\pm p$ are Gauss points of two-point integration. Thus it is expected that the numerical solutions are free from spurious constraints if two-point integration is used.

When 3-point minimization (or integration) is employed, the error-moment equations that minimize the constrained strain energy are given, from Eq. (19), by

$$\int_{-1}^{1}\overline{\gamma_n}d\xi\langle 3:3\rangle=0$$

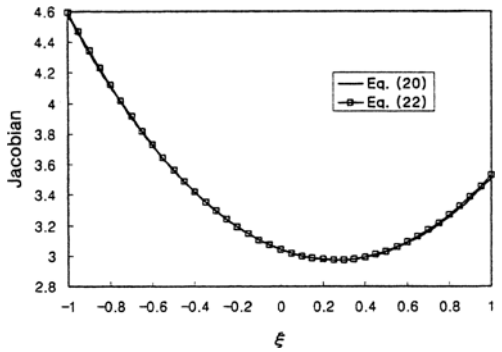

Fig. 5 Jacobian of an out-of-plane-deformable curved beam with a spiral geometry when single element is used

$$\int_{-1}^{1}\overline{\gamma_n}\xi\,d\xi\langle 3:3\rangle=0$$
$$\int_{-1}^{1}\overline{\gamma_n}\xi^2 d\xi\langle 3:3\rangle=0 \tag{32}$$

These equations yield following constraints,

$$\begin{aligned}&\overline{A_0}=0\\&\overline{A_1}+\overline{A_3^*}({}^3\xi_1)^2=0\\&\overline{A_2^*}=0\end{aligned} \tag{33}$$

where the Gauss points of three-pointed integration are 0 and $\pm q$. The first two constraints in Eq. (33) are true constraints and the last one is spurious constraint. Because of the spurious constraint, it is expected that the convergence of numerical solutions will be delayed and the shear stress distribution will be undulate.

So far, we study the constraint condition according to integration rules and Jacobian condition for anisoparametric 3-node element. The results of the analysis based on reduced minimization theory are summarized as follow:

(1) When Jacobian is constant, no spurious constraint is produced irrespective of integration rules.

(2) If the Jacobian is not constant, maximum number of integration points, which does not produce spurious constraints, is two regardless of mapping types.

5. Numerical Test

Test models are the circular model and the spiral model shown in Fig. 2 and Fig. 4, respectively. Both of them are cantilevered curved beams subjected to a concentrated shear force $P=10N$ in the positive binomial direction at the free tip. The material properties are given as follows:

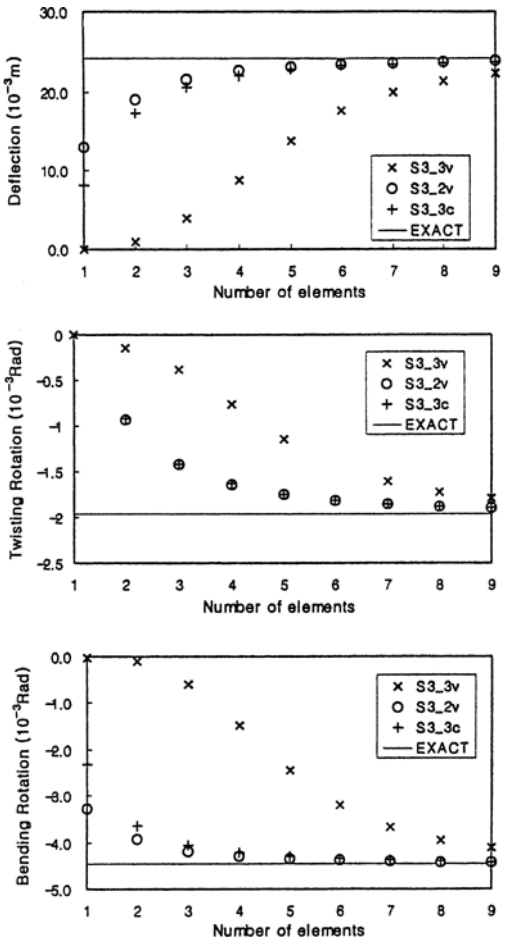

Fig. 6 Displacements of the circular model at $\theta=\pi/2$ are plotted in terms of the number of elements

Young's modulus : $E=2.10\times10^{11}\text{N/m}^2$

Poisson's ratio : $\nu=0.3$

Shear modulus : $G=\dfrac{E}{2(1+\nu)}=8.07\times10^{10}\text{N/m}^2$

Shear correction factor : $k=\dfrac{6(1+\nu)}{7+6\nu}$
≈0.886364

The exact solution of the beams are calculated by Castigliano's theorem. Displacements of the spiral model are calculated by using numerical

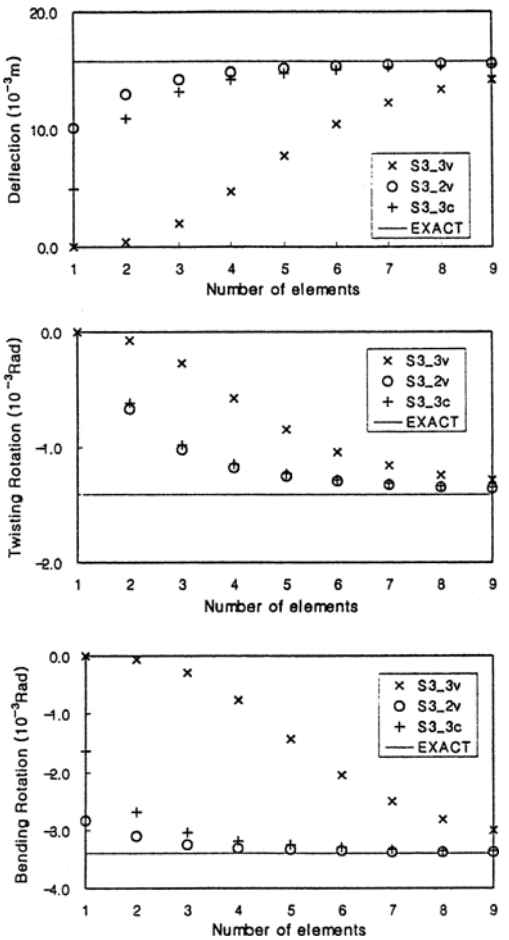

Fig. 7 Displacements of the spiral mdoel at $\theta=\pi/2$ are plotted in terms of the number of elements

integration.

To examine the theoretical predictions on numerical solutions, we perform numerical tests using the following anisoparametric 3-noded elements:

(i) S3_3v which employs 3-point integration for the shear strain.

(ii) S3_2v which employs 2-point integration for the shear strain.

(iii) S3_3c which employs 3-point integration with Jacobian at $\xi=0$ for the shear strain.

All the three elements employ 2-point integration for the calculation of twisting and bending strains. It should be noted that the Jacobian of S3_3v and S3_2v is a function of ξ. But the Jacobian

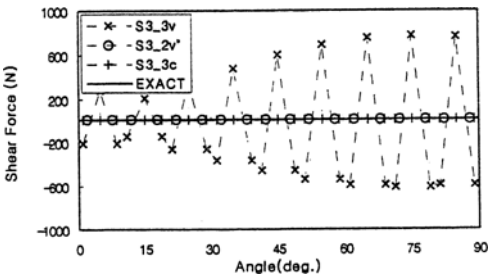

Fig. 8 Distribution of shear stresses of the circular model using nine anisoparametric 3-node elements

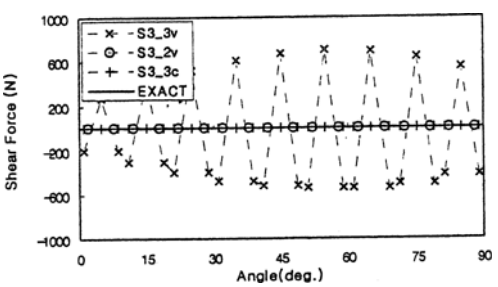

Fig. 9 Distribution of shear stresses of the spiral model using nine anisoparametric 3-node elements

of S3_3c is constant for an element since it uses the Jacobian sampled at $\xi=0$.

5.1 Convergence in terms of number of elements

According to the reduced minimization analysis in the previous section, the element S3_3v produces a spurious constraint while S3_2v and S3_3c yield only true constraints. Thus, the convergence of displacements of S3_3v will be delayed compared with those of S3_2v or S3_3c. To examine this prediction, the displacements at the free tip are plotted in terms of number of elements in Fig. 6 and Fig. 7, which show that the tendency of numerical solutions coincides well with the prediction.

5.2 Undulate stress pattern

The shear stress distribution obtained by S3_3v will be oscillatory since the element yields spurious constraints. But the shear stress distributions obtained by S3_2v and S3_3c will be free from undulate pattern because the element does not

produce spurious constraints. To check this prediction, we plot shear stress distributions along the beam axes in Fig. 8 and Fig. 9 when the beams are discretized by nine elements.

6. Conclusions

This paper presents three-noded, seven DOF, anisoparametric elements (S3_2v and S3_3c) to alleviate the error due to spurious shear constraint. The element of S3_2v uses two-point integration for all strains. The element of S3_3c uses three-point integration with Jacobian at $\xi=0$ for shear strain, and two-point integration for the other strains.

Using the numerical reduced minimization analysis, this paper has shown that the element S3_3v produces a spurious constraint while S3_2v and S3_3c yield only true constraints. Thus, the convergence of numerical displacements of S3_3v is expected to be delayed compared with those of S3_2v or S3_3c. The shear stress distributions of S3_3c will be oscillatory whereas the shear stress distribution of S3_2v and S3_3c will be not. We have shown that the spurious constraint in the element S3_3v arises from the incorporative action of non-constraint Jacobian and 3-point integration.

To confirm the theoretical prediction, numerical tests are performed for circular as well as for non-circular curved beams. The numerical experiments show a good agrement with the theoretical predictions.

Acknowledgement

The authors are grateful for the support provided by Brain Korea 21 from Korea Research Foundation (KPF).

References

Kamoulakos, A., 1988, "Understanding and Improving the Reduced Integration of Mindlin Shell Element," *Int. J. Num. Meth. Engng.*, Vol. 19, pp. 831~840

Kim Yong-woo and Min Oak-key, 1993 "Theoretical Review on the Spurious Modes in Plane Stress/Strain Isoparametric Meshes," *Computers & Structures*, Vol. 49, No. 6, pp. 1069~1082

Kim Yong-woo and Min Oak-key, 1995, "Reduced Minimization in Lagrangian Mindlin Plate with Arbitrary Orientation Under Uniform Isoparametric Mapping," *Int. J. Num. Meth. Engng.*, Vol. 38, No. 12, pp. 2101~2114

Kim Yong-woo and Min Oak-key, 1996, "Optimal Strain Location of Two Dimensional Continuum Elements in Terms of Field-Consistency," *Computers & Structures*, Vol. 59, No. 6, pp. 1121~1138

Kim yong-woo, 1997, "Reuced Minimization of Product and Non-product Type in Mindlin Plate Elements," *Int. J. Num. Meth. Engng.*, Vol. 40, pp. 3117~3139

Kreyszig, E., 1983, *Advanced Engineering Mathematics*, John Wiley & Sons

Martini, L and Vitaliani, R., 1988, "On the Polynomial Convergent Formulation of a C^0 Isoparametric Skew Beam Elements," *Computers & Structures*, Vol. 29, No. 3, pp. 437~449

Min Oak-key and Kim Yong-woo, 1990, "A Consideration of Energy Modes in Isoparametric Quadratic Finite Elements," *Yonsei Nonchong*, Vol. 26, pp. 315~331

Min Oak-key and Kim Yong-woo, 1991, "The Error Due to Spurious Coefficients in Isoparametric Quadratic Beam Element Analysis of Curved Beam Subjected to Out-of-Plane-Loads," *Yonsei Nonchong*, Vol. 27, pp. 231~253

Min Oak-key and Kim Yong-woo, 1994, "Reduced Minimization of Midlin Plate," *Int. J. Num. Meth. Engng.*, Vol. 37, No. 24, pp. 4263~4284

Min Oak-key and Kim Yong-woo, 1994, "Reduced Minimization Theory in Beam Elements," *Int. J. Num. Meth. Engng.*, Vol. 47, pp. 2215~2245

Min Oak-key and Kim Yong-woo, 1996, "Numerical Reduced Minimization Theory for Beam Elements Under Non-Uniform Isoparametric Mapping," *Int. J. Num. Meth. Engng.*, Vol. 39, pp. 1357~1382

Prathap, G. and Babu, C. R., 1986, "An Isopar-

ametric Thick Curved Beam Element," *Int. J. Num. Meth. Engng.*, Vol. 23, pp. 1583~1600

Prathap, G. and Babu, C. R., 1986, "Field-Consistent Strain Interpolation for the Quadratic Shear Flexible Beam Element," *Int. J. Num. Meth. Engng.*, Vol. 23, pp. 1973~1984

Prathap, G. and Babu, C. R., 1987, "Field-Consistency and Violent Stress Oscillations in the Finute Element Method," *Int. J. Num. Meth. Engng.*, Vol. 24, pp. 2017~2033

Prathap, G. and Naganarayama, B. P., 1990, "Analysis of Locking and Stress Oscillations in a General Curved Beam Elements," *Int. J. Num. Meth. Engng.*, Vol. 30, pp. 177~200

Sengupta, D. and Dasgupta, S., 1987, "Horizontally Curved Isoparametric Beam Element with or Without Elastic Foundation Including Effect of Shear Deformation," *Computers & Structures*, Vol. 29, No. 6, pp. 967~973

Sengupta, D. and Dasgupta, S., 1997, "Static and Dynamic Application of a Five Noded Horizontally Curved Beam Element with Shear Deformation," *Int. J. Num. Meth. Engng.*, Vol. 40, pp. 1801~1819

Tessler, A. and Spiridiglozzi, L., 1986, "Curved Beam Elements with Penalty Relaxation," *Int. J. Num. Meth. Engng.*, Vol. 23, pp. 2245~2262

Tessler, A. and Spiridiglozzi, L., 1988, "Resolving Membrane and Shear Locking Phenomena in Curved Shear-Deformable Axisymmetric Shell Elements," *Int. J. Num. Meth. Engng.*, Vol. 26, pp. 1071~1086

Woon-joo Moon, Yong-woo Kim, Oak-key Min and Kang-won Lee, 1986, "Reduced Minimization Theory in Skew Beam Element," *Transactions of the KSME (A)*, Vol. 20, No. 12, pp. 3792~3803

Zienkiewictz, O. C., Taylor, R. L. and Too, J. M., 1971, "Reduced Integration Technique in General Analysis of Plates and Shells," *Int. J. Num. Meth. Engng.*, Vol. 3, pp. 275~290